Enhanced Asymmetric Magnetization Reversal in Nanoscale Co/CoO Arrays: Competition between Exchange Bias and Magnetostatic Coupling

E. Girgis,* R. D. Portugal, H. Loosvelt, M. J. Van Bael, I. Gordon, M. Malfait, K. Temst, and C. Van Haesendonck
Laboratorium voor Vaste-Stoffysica en Magnetisme, Katholieke Universiteit Leuven, Celestijnenlaan 200 D, B-3001 Leuven, Belgium

L. H. A. Leunissen and R. Jonckheere
IMEC vzw, Kapeldreef 75, B-3001 Leuven, Belgium
(Received 19 February 2003; published 30 October 2003)

Magnetization reversal was studied in square arrays of square Co/CoO dots with lateral size varying between 200 and 900 nm. While reference nonpatterned Co/CoO films show the typical shift and increased width of the hysteresis loop due to exchange bias, the patterned samples reveal a pronounced size dependence. In particular, an anomaly appears in the upper branch of the magnetization cycle and becomes stronger as the dot size decreases. This anomaly, which is absent at room temperature in the patterned samples, can be understood in terms of a competition between magnetostatic interdot interaction and exchange anisotropy during the magnetic switching process.

DOI: 10.1103/PhysRevLett.91.187202 PACS numbers: 75.70.Cn, 75.30.Gw, 75.60.Ej, 75.75.+a

Exchange bias (EB) refers to a shift of the magnetization hysteresis loop along the applied field axis and occurs in systems where a ferromagnet (FM) is in atomic contact with an antiferromagnet (AFM) [1]. Usually, the EB shift occurs after cooling the system with a magnetically saturated FM layer below the Néel temperature of the AFM layer. In spite of intensive experimental and theoretical investigation, several aspects of the underlying mechanism still lack a detailed understanding [2–4].

One of the interesting properties of EB is that it produces higher coercive fields when compared to the same FM layers without AFM contact. Exchange-biased systems are therefore very attractive for magnetic storage media where magnetic instability can be a serious drawback. This is, in particular, the case when reducing the magnetic system size down to the nanoscale. Recently, several groups started to investigate the influence of a lateral confinement on the EB effect [5–9].

A remarkable EB feature is the asymmetric magnetization reversal, which was first observed in Fe/FeF_2 and Fe/MnF_2 bilayers [10] and later also investigated in Co/CoO samples [11,12]. In both cases bilayer or multilayer film structures were studied and polarized neutron reflectometry was applied since the reflectometry measurements allow one to discriminate between different magnetization reversal mechanisms. From the neutron experiments it was concluded that different reversal mechanisms are active in the upper and the lower branch of the hysteresis loop. For Fe/FeF_2 and Fe/MnF_2 coherent rotation of the magnetization is proposed for the upper branch and domain wall nucleation and propagation for the lower one, while the opposite occurs in Co/CoO.

In this Letter we report the results of our study of magnetization hysteresis loops for a series of exchange-biased Co/CoO dot arrays where the size of the dots is systematically varied, while leaving the interdot distance constant. Our aim is to study the asymmetric magnetization reversal transition for a confined geometry. We find that varying the size results in a significant change of the magnetic hysteresis loop. Varying the size of the dots gives rise to large changes in the strength of the magnetostatic coupling. We argue that these changes in magnetostatic coupling lead to a pronounced variation of the shape of the upper branch of the hysteresis loop in the exchange-biased state, while the lower branch is less affected. This is directly related to the different nucleation sites (i.e., free surface versus interface) for magnetization reversal for the two branches of the hysteresis loop, where magnetostatic interdot coupling strongly affects the reversal mechanism for the upper branch.

Samples were prepared by dc magnetron sputtering in a high vacuum (base pressure below 8×10^{-8} mbar) sputtering apparatus (Microscience). A Co film with a thickness of 24 nm is deposited at room temperature on predefined resist templates prepared by electron beam lithography on thermally oxidized silicon wafers. The resulting pattern consists of square Co dots with dimensions varying between 200 nm $\times$ 200 nm and 900 nm $\times$ 900 nm and set in a square grid with period varying between 1000 nm and 1700 nm, respectively. The separation between the sides of two neighboring dots is always around 800 nm for the different dot arrays. In order to have a sufficiently large signal for the magnetization measurements, the total area covered by the dot arrays can be increased up to 4 mm $\times$ 4 mm. Next, the Co layer is oxidized *in situ* by exposing the sample to pure oxygen at a pressure of 10^{-4} mbar during 1 h, similar to procedures applied by Gierlings *et al.* [11]. After oxidation the samples are covered with a 3 nm protective gold capping layer and a standard lift-off procedure then allows one to

remove the unwanted parts of the deposited film. Structural characterization with x-ray reflectometry (XRR), scanning electron microscopy (SEM), and atomic force microscopy revealed a low film roughness and a good quality of the patterning. XRR also revealed that the antiferromagnetic CoO layer has a thickness of 2–3 nm. Low temperature magnetization hysteresis loops were measured by a superconducting quantum interference device (SQUID) based magnetometer (Quantum Design, MPMS) and by a vibrating sample magnetometer (VSM, MagLab, Oxford Instruments). All hysteresis loops are normalized by the experimentally determined saturation magnetization M_S to take into account the different areas of magnetic material in the different samples.

Figure 1 shows the unidirectional hysteresis loop shift for an exchange-biased Co/CoO reference (nonpatterned) film measured by the SQUID magnetometer at 10 K after field cooling in a field of +0.4 T. Both the shape of the loop and the magnitude of the EB shift are in good agreement with observations made by many groups. Figure 2 shows the SEM images of the studied square dot arrays with dot size of 900 nm (a), 800 nm (b), 400 nm (c), and 200 nm (d), respectively. The center-to-center distances are 1700 nm (a), 1600 nm (b), 1200 nm (c), and 1000 nm, respectively. Figure 3 shows the low temperature hysteresis loops for the Co/CoO dots with a dot size of 900 nm (a), 800 nm (b), 400 nm (c), and 200 nm (d), respectively. The loops are measured after cooling the dot arrays in an in-plane magnetic field of +0.4 T, applied parallel to the side of the dots. Loop (c) was measured at a temperature of 10 K, while the other loops were measured at 5 K. Loop (b) was obtained by the SQUID, while the other loops were measured by the vibrating sample magnetometer. All loops were corrected by subtraction of the diamagnetic background caused by the substrate. The more reliable determination of zero magnetization for the SQUID measurements allows one to identify the presence of small vertical shifts of the hysteresis loops [13], which may be linked to the freezing of uncompensated spins in the AFM layer [14].

The magnetization curves in Fig. 3 reveal an asymmetry which strongly depends on the magnetic dot size. A small shoulder appears in the upper branch of the magnetization curve in Fig. 3(a), and this shoulder (indicated by the arrows in Fig. 3) becomes more pronounced as the size of the dots is reduced, leading to an apparent destruction of the EB effect for the smallest dots in Fig. 3(d). While the magnetization loop in Fig. 3(d) is still asymmetric about zero field, the hysteretic behavior extends towards higher fields for the smallest dot size. Figure 3(d) also suggests that the EB is suppressed for the smallest structures, in agreement with earlier observations [5,9]. Our magnetic force microscopy (MFM) measurements (not shown) indicate that the largest dots have a multidomain structure, implying that the domain wall configuration is able to adjust to internal and external magnetic fields. Our MFM images did not allow us to identify the domain structure in the smaller dots, but we expect the presence of a single-domain configuration and, hence, a switching characteristic different from the larger dots. A lateral size of 200 nm was found to be below the critical size for single-domain formation [15], although this critical dimension may change due to the presence of the antiferromagnet. The hysteresis loops in Fig. 3 should be compared to the loop of the reference film in Fig. 1, where no such anomaly is present in the upper magnetization curve. Except for the smallest dot size, the lower branch of the hysteresis loops in Fig. 3 shows no appreciable change in shape. As discussed in more detail below, we believe this peculiar behavior arises from the competition between the magnetostatic interdot interaction energy and the exchange anisotropy energy at the FM/AFM interface.

As shown before [16], arrays of magnetically coupled dots reveal internal switching asymmetries. When combined with the typical unidirectional anisotropy of the EB in our samples, the magnetic coupling allows one to understand the magnetic response of our dot arrays. Similar to the case of dot arrays where EB is absent, switching in the array is expected to start before the external field reaches zero due to the presence of the

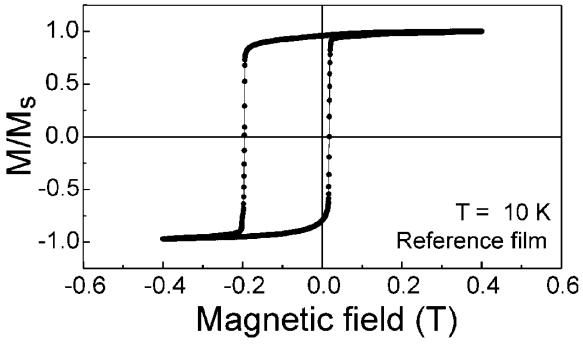

FIG. 1. Hysteresis loop of a reference (i.e., nonpatterned) Co/CoO film measured after field cooling at +0.4 T.

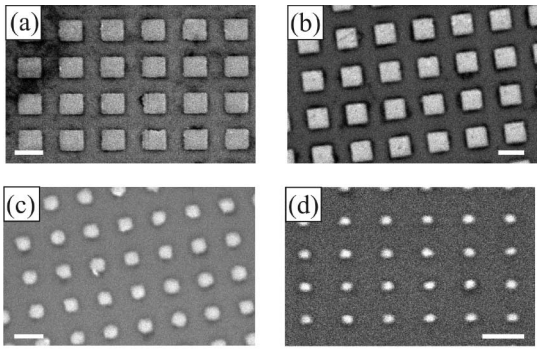

FIG. 2. SEM images of the Co/CoO square dot arrays. The white marker corresponds to a length of 1 μm.

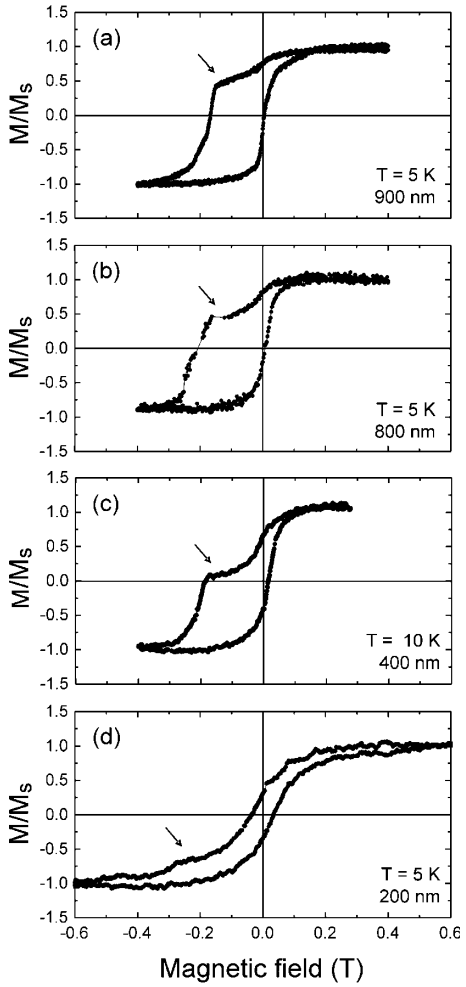

FIG. 3. Hysteresis loops of the Co/CoO square dot arrays with four different dot sizes. All magnetization curves have been measured after cooling the array in a magnetic field of +0.4 T. The arrow indicates the position of the intermediate saturation in the upper branch of the hysteresis loop which may be linked to the magnetostatic coupling between the dots.

interaction between dots. On the other hand, none of our samples show zero magnetization at zero external field. Such a zero remanence is typical of magnetic dots with strong magnetostatic coupling [17]. In our dot arrays EB produces an additional barrier that has to be overcome and causes a nonzero remanence. The largest difference between samples with different dot size occurs in the vicinity of the remanent state, where the decay rate of the magnetization is clearly different for the four investigated samples. If we assume that magnetization reversal initially proceeds via one-by-one switching of the magnetization of the dots, the arrays with larger (more strongly coupled) dots are expected to reveal an intermediate saturation of the magnetization reversal (see the arrows in Fig. 3) before the total switching occurs. A larger dot produces a higher stray field in its vicinity when compared to a smaller dot. Consequently, once the magnetization of a larger dot is reversed, this tends to stabilize the magnetization of its nearest neighbors. Switching of other dots in the immediate vicinity of the dot that switched first is inhibited, and the intermediate saturation occurs earlier for larger dot sizes. For the smallest dots the interdot magnetostatic interaction becomes relatively weak and rotation of individual dots has less influence on the subsequent switching of the remaining dots. The stability of a dot is therefore determined by the relative magnitude B_i/B_{ref} of the magnetostatic field felt by each dot at the switching point due to the interaction with its nearest neighbors and can be calculated as follows:

$$\frac{B_i}{B_{\mathrm{ref}}} = \frac{f(a_i, b_i)}{f(a_{\mathrm{ref}}, b_{\mathrm{ref}})}, \tag{1}$$

where the function $f(a, b)$ is defined as

$$f(a, b) = \frac{2(2b + a)}{\sqrt{a^2 + (2b + a)^2}} - \frac{2(2b - a)}{\sqrt{a^2 + (2b - a)^2}}, \tag{2}$$

with a the square dot size and b the distance between the centers of adjacent dots (i.e., the period of the array). B_{ref} is the magnetostatic field felt by the smallest dots (200 nm $\times$ 200 nm). In Table I the relative magnitudes of the magnetostatic fields calculated from Eqs. (1) and (2) are given for the four different dot sizes.

In order to further illustrate the relevance of the asymmetry of the magnetization reversal mechanism we rely on a simple physical picture inferred from the theoretical modeling of EB at the ferromagnetic monolayer level [18]. In Fig. 4 magnetic dots are represented as a stack of monolayers with a spin magnetization given by the arrow in each of the monolayers. The white arrow in the top layer refers to the direction of the exchange anisotropy imposed by the cooling field in the AFM, i.e., the fixed direction of the magnetization in the layer of the CoO closest to the FM/AFM interface.

Figure 4(a) illustrates the evolution of the ferromagnetic spin magnetization for the upper part of the hysteresis loops. The left picture shows the spin configuration for positive magnetic fields. Ferromagnetic spins feel perfectly "comfortable" with the exchange anisotropy generated at the FM/AFM interface. When the field is lowered, magnetization reversal starts at the bottom

TABLE I. Relative magnitude of the magnetostatic fields of the square dot arrays with different size a and center-to-center distance b.

a (nm)	b (nm)	B_i/B_{ref}
200	1000	1
400	1200	4.66
800	1600	15.89
900	1700	18.96

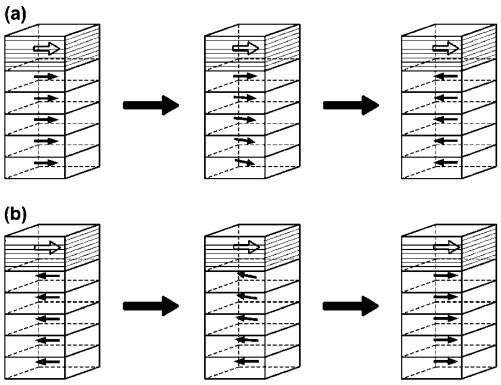

FIG. 4. Schematic representation of the model accounting for the magnetization reversal in the patterned Co/CoO structures. The upper (lower) row of spin configurations illustrates the magnetization reversal mechanism in the FM layer for the upper (lower) branch of the hysteresis loops. The FM layer is represented as a stack of monolayers with a spin magnetization given by the arrow in each of the monolayers. The upper white arrow represents the direction of the exchange anisotropy imposed by the AFM layer.

layer, i.e., the most unstable spin monolayer, and propagates up to the interface until full reversal is achieved. The driving force behind the bottom layer rotation is the decrease in Zeeman energy resulting from the interplay between the externally applied field and the interdot magnetostatic interaction. For larger dots the bottom monolayer is more unstable (larger interdot interaction), but once one dot is reversed, it is able to stabilize a larger number of neighboring dots, implying that subsequent dot rotation becomes more difficult. Consequently, different dot sizes result in different magnetization curves.

Figure 4(b) illustrates the magnetization reversal for the lower branch of the magnetization curve. In the left picture the ferromagnetic spins are aligned along the external negative magnetic field. In this case the FM monolayer next to the FM/AFM interface is the most unstable, because it is frustrated with the spin configuration of the lower AFM layer. When the external field is reduced (less negative), the Zeeman energy is decreased and the frustrated FM monolayer will be the first to start moving. Since the interface frustration is the driving force determining the lower branch of the magnetization loop, the switching of each Co dot can proceed in a similar fashion, almost independently of the rotation of its neighbors, explaining why the bottom branches of the magnetization loops do not appreciably depend on the dot size.

In conclusion, the asymmetry of the magnetization curves for exchange-biased magnetic dots was investigated for different dot sizes. The evolution of the asymmetry of the hysteresis loops with decreasing dot size can be understood in terms of a balance between the magnetostatic interdot interaction energy and the exchange anisotropy energy. The striking observation that the two branches of the hysteresis loop are affected in a fundamentally different way is therefore linked to our ability to tune the magnetostatic interaction between the dots. This procedure allows to probe the influence of magnetostatic interactions, not only on the exchange bias effect, but on magnetization reversal transitions in general.

The authors thank V.V. Moshchalkov for enlightening discussions and M. Rots and B. Croonenborghs for their help with some of the magnetization measurements. This work was supported by the Fund for Scientific Research–Flanders (FWO) as well as by the Belgian Interuniversity Attraction Poles (IAP) and the Flemish Concerted Action (GOA) programs. R. D. P. acknowledges additional support from the Flanders-Chile Bilateral Agreement No. BIL00/01.

*Electronic address: Emad.Girgis@NRC-edu.eg

[1] W. P. Meiklejohn and C. P. Bean, Phys. Rev. **102**, 1413 (1956).
[2] J. Nogués and I. K. Schuller, J. Magn. Magn. Mater. **192**, 203 (1999).
[3] A. E. Berkowitz and K. Takano, J. Magn. Magn. Mater. **200**, 552 (1999).
[4] M. Kiwi, J. Magn. Magn. Mater. **234**, 584 (2001).
[5] M. Fraune, U. Rüdiger, G. Güntherodt, S. Cardoso, and P. Freitas, Appl. Phys. Lett. **77**, 3815 (2000).
[6] S. Zhang and Z. Li, Phys. Rev. B **65**, 054406 (2001).
[7] K. Liu, S. M. Baker, M. Tuominen, T. P. Russell, and I. K. Schuller, Phys. Rev. B **63**, 060403 (2001).
[8] T. Pokhil, D. Song, and E. Linville, J. Appl. Phys. **91**, 6887 (2002).
[9] Y. Shen, Y. Wu, H. Xie, K. Li, J. Qiu, and Z. Guo, J. Appl. Phys. **91**, 8001 (2002).
[10] M. R. Fitzsimmons, P. Yashar, C. Leighton, I. K. Schuller, J. Nogués, C. F. Majkrzak, and J. A. Dura, Phys. Rev. Lett. **84**, 3986 (2000).
[11] M. Gierlings, M. J. Prandolini, H. Fritzsche, M. Gruyters, and D. Riegel, Phys. Rev. B **65**, 92407 (2002).
[12] F. Radu, M. Etzkorn, R. Siebrecht, T. Schmitte, K. Westerholt, and H. Zabel, Phys. Rev. B **67**, 134409 (2003).
[13] J. Nogués, C. Leighton, and I. K. Schuller, Phys. Rev. B **61**, 1315 (2000).
[14] J. Keller, P. Miltényi, B. Beschoten, G. Güntherodt, U. Nowak, and K. D. Usadel, Phys. Rev. B **66**, 14 431 (2002).
[15] O. Kazakova, M. Hanson, P. Blomquist, and R. Wäppling, J. Appl. Phys. **90**, 2440 (2001).
[16] R. E. Dunin-Borkowski, M. R. McCartney, B. Kardynal, David J. Smith, and M. R. Scheinfein, Appl. Phys. Lett. **75**, 2641 (1999).
[17] V. Novosad, K. Yu. Guslienko, H. Shima, Y. Otani, S. G. Kim, K. Fukamichi, N. Kikuchi, O. Kitakami, and Y. Shimada, Phys. Rev. B **65**, 060402 (2002).
[18] M. Kiwi, J. Mejía-López, R. D. Portugal, and R. Ramírez, Appl. Phys. Lett. **75**, 3995 (1999).